J. Fluid Mech. (2005), vol. 529, pp. 51–69.
doi:10.1017/S0022112004002940 Printed in the United Kingdom

Lift, thrust and heat transfer due to mixed convection flow past a horizontal plate of finite length

By WILHELM SCHNEIDER

Institut für Strömungslehre und Wärmeübertragung, Technische Universität Wien, Resselgasse 3/322, A-1040 Vienna, Austria
wilhelm.schneider@tuwien.ac.at

(Received 4 October 2003 and in revised form 14 October 2004)

The steady two-dimensional mixed-convection flow past a heated or cooled horizontal plate of finite length is analysed for large Péclet numbers and weak buoyancy effects. The plate is assumed to be aligned with the free stream. It is shown that the hydrostatic pressure jump across the wake, combined with the Kutta condition, gives rise to a potential flow that can be determined by distributing vortices in the wake as well as in the plate. Solutions in closed form are obtained for two cases, i.e. laminar flow of a fluid with very small Prandtl number and turbulent flow. As a result, a lift force opposite to the buoyancy force and a tangential force opposite to the viscous drag force are found. For the case of laminar flow of a fluid with very small Prandtl number, closed-form solutions are also obtained for the temperature distribution and the heat transfer rate, respectively.

1. Introduction

The paper concerns the effects of weak buoyancy on the flow past a horizontal, heated or cooled plate that is aligned with the free stream. As the tangential component of the gravity force vanishes in this case, buoyancy affects the flow primarily via the hydrostatic pressure gradient in the thermal boundary layer. This indirect buoyancy effect has been investigated by several authors (cf. Schlichting & Gersten 2000; Schneider 2001; Steinrück 2001 for recent surveys), assuming – often tacitly – a plate of semi-infinite extent, apparently with the understanding that, owing to the parabolic nature of the boundary-layer equations, the results would also apply to a plate of finite length, say L. This may indeed be true if one surface of the plate is heated, while the other one is cooled such as to obtain a symmetric flow field (Robertson, Seinfeld & Leal 1973); but in the more common case of a finite plate that is either heated or cooled at both surfaces, there is an additional effect that is primarily due to the hydrostatic pressure difference across the wake, as was noted recently (Schneider 2000). Continuity of pressure requires the pressure difference across the wake to be compensated by an outer potential flow superimposed on the free stream, cf. figure 1. This potential flow may be represented by a continuous vortex distribution in the wake and in the plate.

The vortex distributions are associated with circulation, and a potential flow with circulation gives rise to a (positive or negative) lift force, i.e. a normal force acting on the plate in the direction opposite to the buoyancy force. Furthermore, in an analogy to the well-known aerodynamic problem of an inclined flat plate, there is

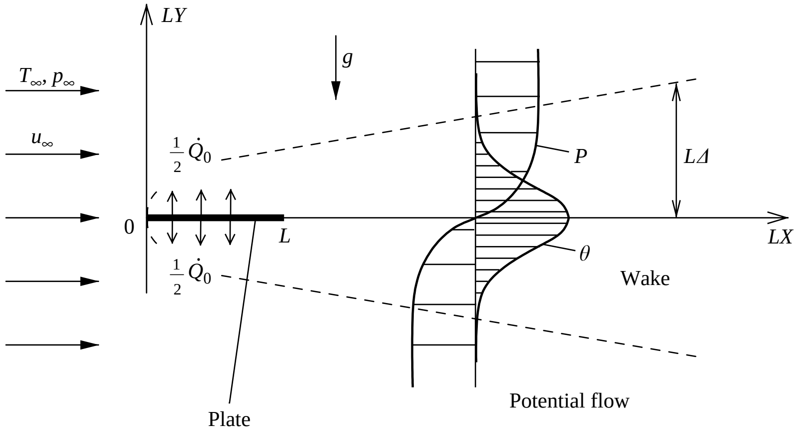

FIGURE 1. Temperature perturbation, θ, and pressure perturbation, P, in the wake behind a heated horizontal plate of finite length (schematic).

also a tangential force due to the so-called leading-edge suction. According to the analysis given by Oswatitsch (1976), this force is acting in the direction opposite to the free-stream velocity.

It is obvious that the induced potential flow will also affect the heat transfer at the plate. Since the pressure perturbations associated with the potential flow and the hydrostatic pressure perturbations must have opposite signs, we might expect that the effect of buoyancy on the heat transfer is reduced, perhaps even reversed, as a result of the induced flow. The analysis will show, however, that the effect of the induced flow on the heat transfer is more subtle than it appears at the first glance.

The present paper is organized as follows. Upon presenting the basic assumptions in § 2, the induced potential flow and the forces associated with it are considered in § 3. The results of § 3 are based on assumptions that apply equally well to the laminar flow of a fluid with very small Prandtl number, e.g. a liquid metal, and to a turbulent flow with very large Reynolds number. The heat transfer problem is considered in § 4. Since a treatment of the thermal boundary layer in turbulent flow is not possible without recourse to turbulence modelling, the analysis of § 4 is restricted to laminar flow.

2. Basic assumptions

To make a solution in closed form feasible, we shall apply the Boussinesq approximation and assume that the fluid velocity – in the case of turbulent flow: the mean flow velocity – differs little from the constant free-stream value, u_∞, both in the potential flow and in the thermal wake, except in a very thin viscous sub-layer. This assumption is justified if the following conditions are satisfied:

(i) Weak buoyancy effects, i.e. $Ri \ll 1$, where Ri is a Richardson number in terms of the heat supplied at the plate, per unit of time, cf. the definition given below. This condition not only simplifies the analysis, it is also a necessary condition for preventing boundary-layer separation (cf. Robertson *et al.* 1973; Higuera 1997) and/or the onset of secondary-flow vortices in the boundary layer (cf. Wu & Cheng 1976; Imura, Gilpin & Cheng 1978; Moutsoglou, Chen & Cheng 1981; Wang 1982; Hall & Morris 1992; Lee, Chen & Armaly 1992). For weak buoyancy effects we may, furthermore, discard the peculiar singularities that were apparently first observed by Schneider & Wasel (1985) and are now known to be associated with eigensolutions (Steinrück 1994) and the existence of sub-layers (Lagrée 2001). Finally, by analogy to the classical problem of incompressible flow past a flat plate at incidence (Brown & Stewartson 1970; Chow & Melnik 1976; Smith 1983; cf. also the survey by Kluwick 1998), the assumption of small perturbations provides a basis for applying the Kutta condition at the trailing edge.

(ii) Either laminar flow of a fluid with very small Prandtl number Pr, or turbulent flow with very large Reynolds number Re, with $Re = \rho_\infty u_\infty L/\mu$, where ρ_∞ is the constant free-stream value of the fluid density and μ is the constant viscosity of the fluid. In the former case, the viscous sub-layer occupies only a fraction as small as $\sqrt{Pr}$ of the thermal wake, as in any thermal boundary layer (cf. Schlichting & Gersten 2000, p. 217). In the latter case, the mean velocity defect in the bulk of the near wake is of the order of the friction velocity, which is as small as $1/\ln(Re)$ as compared to the free-stream velocity, while the ratio of the thickness of the viscous sub-layer to that of the defect layer is as small as $Re^{-1}\ln(Re)$, cf. Schlichting & Gersten 2000, p. 576. For more details, see Kluwick (1998, pp. 302–311). As $x \to \infty$, the velocity defect in the wake decays, justifying the assumption of small mean velocity perturbations ever better. Note also that it is not necessary that the whole boundary layer at the plate is turbulent. Laminar and/or transitional regions in the front part of the plate are admissible provided the turbulent flow develops into a defect layer and a thin viscous sub-layer before it reaches the trailing edge.

3. Flow induced by the thermal wake

3.1. *Non-dimensional variables*

In § 3, the following non-dimensional variables are used. The Cartesian coordinates x and y refer to the plate length L, while the velocity components u and v (in the direction of x and y, respectively) refer to the free-stream velocity, u_∞. Furthermore, the pressure difference with respect to the ambient pressure refers to twice the stagnation pressure, i.e. $\rho_\infty u_\infty^2$. This non-dimensional pressure difference is denoted by p. To discriminate between the potential flow and the wake flow, capital letters (i.e. X, Y, U and P) are used for the latter region without changing the reference quantities, with the exception of Y, which is defined as $Y = y/\Delta$, where $\Delta = \Delta(x)$ characterizes the half-thickness of the thermal wake in terms of the plate length, cf. figure 1. There are, of course, various ways of defining Δ, but this is of no relevance for the present analysis. In addition, the non-dimensional temperature difference $\theta = (T - T_\infty)/T_\infty$ is introduced, with T_∞ as the constant temperature of the free stream. In the case of turbulent flow, all flow variables, i.e. velocity, pressure and temperature, are to be understood as time-averaged quantities.

3.2. *Integral relationships for the wake* ($X > 1$)

In the framework of the Boussinesq approximation, only two forces contribute to the pressure difference across the wake, i.e. hydrostatic forces and centrifugal forces. The pressure perturbation due to centrifugal forces is of the order of $\kappa\rho_\infty u_\infty^2(U^2 - u^2)\Delta$, where κ is the non-dimensional curvature of the wake centreline. Since the wake curvature is solely due to buoyancy forces, the curvature is very small for small Richardson numbers. On the other hand, the velocity perturbation in the wake is also small. Thus, the contribution of the centrifugal forces is small at higher order, and the pressure difference across the wake is, in a first approximation, equal to the hydrostatic one, i.e.

$$\rho_\infty u_\infty^2 [P(X,+\infty) - P(X,-\infty)] = g\rho_\infty \beta T_\infty L\Delta \int_{-\infty}^{+\infty} \theta \,\mathrm{d}Y \qquad (X \geqslant 1), \tag{1}$$

where g denotes the acceleration due to gravity and β the (constant) thermal expansivity of the fluid.

The integral appearing on the right-hand side of (1) may be related to the heat flow rate $\dot{Q}$, i.e. the heat supplied at the plate per units of time and width. Neglecting dissipation (cf. Appendix A for justification), the over-all energy balance gives

$$\rho_\infty u_\infty c_p T_\infty L\Delta \int_{-\infty}^{+\infty} U\theta \,\mathrm{d}Y = \dot{Q}, \tag{2}$$

with c_p being the isobaric specific heat capacity of the fluid. According to the assumption of small velocity disturbances, U may be replaced by 1 in a first approximation. Furthermore, in view of the assumption of weak buoyancy effects we may replace $\dot{Q}$ by $\dot{Q}_0$, which is the heat flow rate due to forced convection under equal conditions. Combining (1) and (2), we then obtain

$$P(X,+\infty) - P(X,-\infty) = Ri \qquad (X \geqslant 1), \tag{3}$$

where Ri is a Richardson number defined in terms of the heat flow as follows:

$$Ri = \frac{g\beta \dot{Q}_0}{c_p \rho_\infty u_\infty^3}. \tag{4}$$

Replacing $\dot{Q}$ by $\dot{Q}_0$ is, of course, of relevance only if the heat flow is not given, e.g. in the case of a given plate temperature. In this case, well-known heat transfer relationships (cf. Schlichting & Gersten 2000, pp. 215–218 for laminar flow with $Pr \to 0$ and pp. 604–606 for turbulent flow, respectively) can be applied to determine $\dot{Q}_0$.

Equation (3) shows that the hydrostatic pressure difference across the wake is constant. It also shows that the effects of buoyancy are weak if $Ri \ll 1$, as has been anticipated with condition (i) in § 2.

3.3. *Potential flow*

The hydrostatic pressure difference across the wake is to be compensated by a potential flow that satisfies the matching condition

$$p(x,0\pm) = P(X,\pm\infty) \qquad (x, X \geqslant 1). \tag{5}$$

The overall hydrostatic pressure difference across the wake is already known from (3); but the Kutta condition requires compensation of the hydrostatic pressure perturbation on each side of the plate as the trailing edge is approached. In this paper, we shall consider the common cases of equal temperature distributions or equal heat flux distributions at the upper and lower sides of the plate, respectively. Half of the total heat flow rate $\dot{Q}_0$ is then supplied at each side of the plate, cf. figure 1, and for symmetry reasons the matching condition (5) together with (3) becomes

$$p(x,0\pm) = \pm\tfrac{1}{2} Ri \qquad (x \geqslant 1). \tag{6}$$

Other cases of possible interest, such as the case of all the heat supplied at one side of the plate while the other one is adiabatic, can be treated in a similar manner, if required.

At the plate the potential flow has to satisfy the boundary condition

$$v(x,0\pm) = 0 \qquad (0 < x < 1), \tag{7}$$

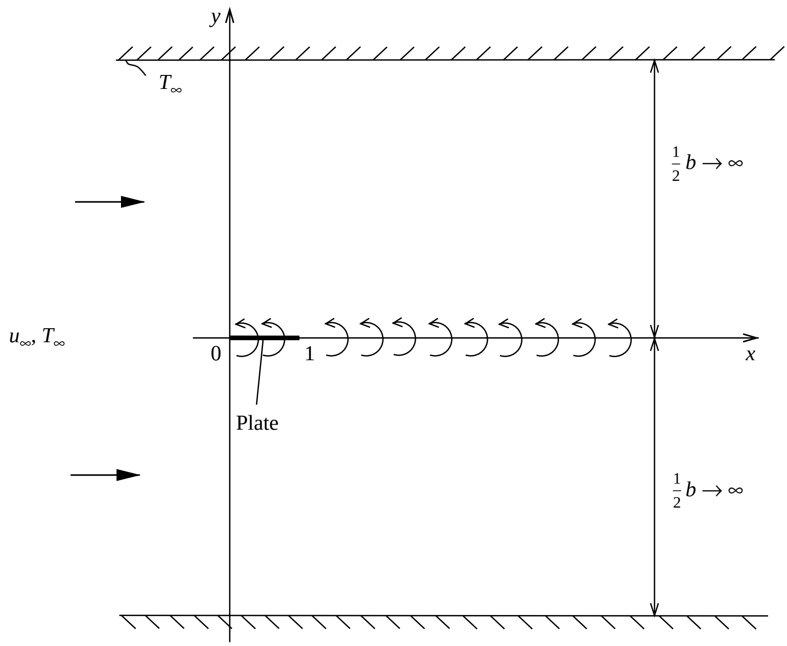

FIGURE 2. Plate in channel of width b, with $b=(2/\pi)|Ri|^{-n}\rightarrow\infty$ as $Ri\rightarrow 0$, and vortex distribution (schematic).

expressing tangential flow. Displacement due to the viscous boundary layer is discarded as a higher-order effect that can be superimposed, if required.

In what follows, the potential-flow solution will be given in terms of the strength of vortices distributed continuously in the plane of the plate, i.e. along the x-axis, both in the plate ($0<x<1$) and in the wake region ($x\geqslant 1$) (figure 2). The curvature of the wake is neglected on the basis of the assumption of small disturbances.

According to a classical result of potential-flow theory, the vortex strength of a plane vortex sheet is equal to twice the pressure perturbation at the sheet. Thus, (6) requires a constant vortex strength in the wake region ($x\geqslant 1$). However, applying Biot-Savart's law shows that a vortex sheet of constant strength induces velocities that grow beyond bounds as the sheet extends from a fixed initial point, i.e. $x=1$, to infinity. A similar difficulty is encountered with semi-infinite sink distributions of constant strength, representing the entrainment into a plane turbulent plume (Taylor 1958) or into a plane turbulent mixing layer (Mörwald 1988). The most obvious means of dealing with these difficulties is to introduce bounds to the flow field, e.g. a horizontal wall in the case of the plume (Taylor 1958; Schneider 1991) or a plane of sources that represents the origin of the free streams in the case of the mixing layer (Schneider 1991). In a previous investigation of the present problem (Schneider 2000), the difficulty was circumvented by assuming that the vertical velocity component vanishes at a large, but finite, distance upstream of the leading edge of the plate. Bounding the flow field in that way is not quite satisfactory, however, since it leads to a first-order perturbation of the horizontal velocity component at the upstream boundary.

In the present paper, another approach is pursued. We consider a flow field that is bounded by plane walls parallel to the plate, as indicated in figure 2, assuming that

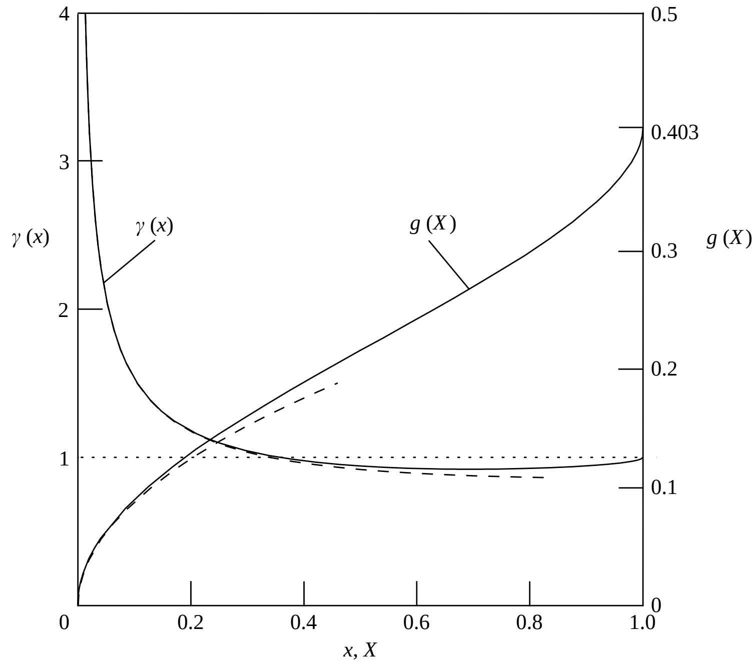

FIGURE 3. The functions $\gamma(x)$ and $g(X)$ according to (10) and (45), respectively (solid lines). Also shown: asymptotic expansions for $x \ll 1$ and $X \ll 1$ according to (12) and (50), respectively (dashed lines).

the channel width b, referred to the plate length, tends to infinity as the Richardson number Ri tends to zero. To be specific, we put $b = (\pi/2)|Ri|^{-n}$, with $n = \text{const} > 0$ and the coefficient $\pi/2$ being introduced for later convenience. This appears to be a formulation of the problem that resembles the unbounded domain, including the downstream region (see Appendix D), as closely as possible. Besides, it may also provide a suitable basis for a numerical solution of the problem, which is, however, beyond the scope of the present work.

The solution to this problem can be found by conventional methods of potential-flow theory, e.g. by applying the mirror method together with Biot-Savart's law, or by introducing a complex potential. Details of the analysis may be found in Appendix B. Here, it suffices to supply the results for the distributions of pressure and velocity, respectively, at the plate. The following asymptotic representation for $Ri \to 0$ is obtained:

$$p(x, 0\pm) = \mp \frac{n}{2\pi} Ri \ln |Ri| \sqrt{\frac{1-x}{x}} \pm \tfrac{1}{2} Ri\, \gamma(x), \qquad (8)$$

$$u(x, 0\pm) = 1 - p(x, 0\pm), \qquad (9)$$

with

$$\gamma(x) = \frac{1}{\pi^2} \sqrt{\frac{1-x}{x}} \int_0^1 \sqrt{\frac{\xi}{1-\xi}} \ln(1-\xi) \frac{d\xi}{x-\xi} \qquad (0 < x < 1). \qquad (10)$$

The Cauchy principal value of the integral is to be taken in the latter equation. The integral can be evaluated with standard numerical methods. The result is shown in figure 3. As $x \to 1$, i.e. as the trailing edge is approached, $\gamma(x)$ tends to the value 1, see

Appendix C. At the leading edge, the potential-flow solution is singular. Expanding (10) for small values of x and making use of the integral formulae (according to '*Mathematica*')

$$\int_0^1 \frac{\ln(1-\xi)}{\sqrt{\xi(1-\xi)}}\,\mathrm{d}\xi = -2\pi\ln 2, \qquad \int_0^1 \frac{\ln(1-\xi)}{\xi\sqrt{\xi(1-\xi)}}\,\mathrm{d}\xi = -2\pi \tag{11}$$

gives

$$\gamma(x) = \frac{1}{\pi}\left[\frac{2\ln 2}{\sqrt{x}} + (2-\ln 2)\sqrt{x} + \ldots\right]. \tag{12}$$

It might be of interest to observe that the first term on the right-hand side of (8) resembles the pressure perturbation for the classical problem of forced flow past a flat plate at an angle of attack that has the small value $-(nRi/2\pi)\ln|Ri^{-1}|$.

3.4. *Lift force and force due to leading-edge suction*

The pressure due to the potential flow with circulation gives rise to a normal force acting on the plate, i.e. a lift force. Accounting for the contributions from both the upper and lower surfaces of the plate and, as usual, referring the force to the free-stream stagnation pressure and to the plate area, we obtain for the lift coefficient, C_L, the relationship

$$C_L = -4\int_0^1 p(x, 0+)\,\mathrm{d}x. \tag{13}$$

Substituting for $p(x, 0+)$ according to (8) and performing the integration gives

$$C_L = -Ri\left[-n\ln|Ri| + 2\int_0^1 \gamma\,\mathrm{d}x\right] \tag{14}$$

with

$$\int_0^1 \gamma\,\mathrm{d}x = 1.193 \tag{15}$$

obtained from a numerical integration based on the result (10). Since $\ln|Ri|$ is negative for small values of Ri, it follows from (14) that the lift force is in the opposite direction to the buoyancy force, i.e. the lift force points downward for a heated plate, provided the thermal expansivity is positive. The lift coefficient as a function of the Richardson number according to (14) and (15) is shown in figure 4.

The lift force is not the only force induced by the vortex distribution. In addition there is a tangential force due to the potential flow around the leading edge of the plate ('leading-edge suction'). According to Oswatitsch (1976), the tangential force coefficient associated with a tangential velocity perturbation $\varepsilon/\sqrt{x}$ (as $x \to 0$, with $\varepsilon = \mathrm{const}$) in incompressible flow is $C_S = -2\pi\varepsilon^2$. Expanding (8) for small values of x and making use of (9), (11) and (12) gives

$$C_S = -\frac{Ri^2}{2\pi}[-n\ln|Ri| + \ln 4]^2. \tag{16}$$

Note that $C_S < 0$, indicating a force in the opposite direction to the free stream, i.e. a 'thrust', irrespective of whether the plate is heated ($Ri > 0$) or cooled ($Ri < 0$). The coefficient C_S as a function of the Richardson number according to (16) is also shown in figure 4.

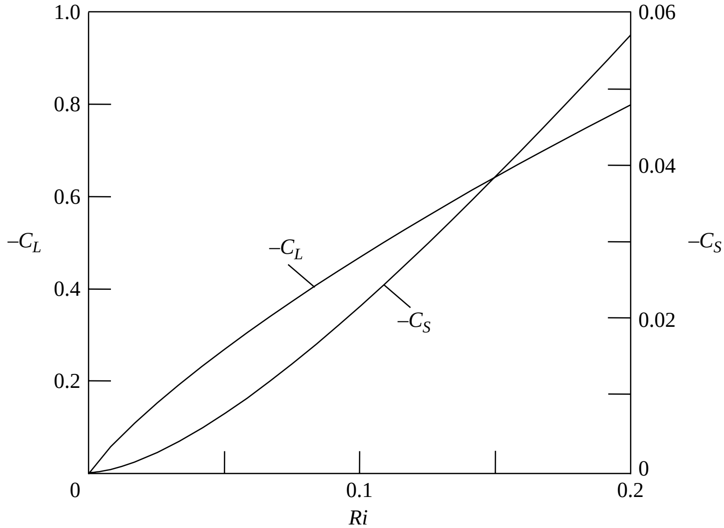

FIGURE 4. Lift coefficient, C_L, and tangential force coefficient due to leading-edge suction, C_S, as functions of the Richardson number, Ri, for $n = 1$.

4. Thermal boundary layer at the plate

4.1. *Non-dimensional variables, basic equations and asymptotic expansions*

The following analysis concerns the effects of weak buoyancy on the two-dimensional thermal boundary layer at a horizontal plate of constant surface temperature T_p, which differs from the constant temperature T_∞ in the free stream of constant velocity u_∞. For reasons discussed in § 1, the limiting case of vanishing Prandtl number is considered. In this case, the thermal boundary layer is inviscid, apart from a very thin viscous sub-layer, whose effect on the heat transfer may be neglected (cf. Hieber 1973; Leal 1973; Wickern 1991).

The variables describing the boundary-layer flow are denoted by capital letters. While the tangential components as well as the pressure difference remain unchanged, i.e. $X = x$, $U = u$, $P = p$, the normal components are stretched according to

$$Y = y\sqrt{Pe}, \qquad V = v\sqrt{Pe}, \tag{17}$$

where $Pe = u_\infty L/\alpha$ is the Péclet number, with α as thermal diffusivity of the fluid. For symmetry reasons, it suffices to consider only the upper surface of the plate, i.e. $Y \geqslant 0$.

In addition, the non-dimensional temperature difference

$$\Theta = (T - T_\infty)/(T_p - T_\infty) \tag{18}$$

is introduced. Note that Θ is related to the previously introduced variable θ according to $\Theta = \theta T_\infty/(T_p - T_\infty)$.

The basic equations are the boundary-layer equations governing mixed-convection flow over horizontal surfaces (cf. Gersten & Schilawa 1978; Gersten & Herwig 1992, pp. 284–289). The viscous terms can be dropped for vanishing Prandtl number to obtain the following non-dimensional form of the boundary-layer equations for inviscid flow (with subscripts X and Y indicating partial derivatives with respect to

X and Y, respectively):

$$U_X + V_Y = 0, \tag{19}$$

$$UU_X + VU_Y + P_X = 0, \tag{20}$$

$$P_Y = (Ar/\sqrt{Pe})\Theta, \tag{21}$$

$$U\Theta_X + V\Theta_Y = \Theta_{YY}, \tag{22}$$

where $Ar = g\beta(T_p - T_\infty)L/u_\infty^2$ is the Archimedes number. The appropriate boundary conditions are

$$V(X, 0) = 0, \quad \Theta(X, 0) = 1, \tag{23}$$

$$U(X, \infty) = u(x, 0+), \quad P(X, \infty) = p(x, 0+), \quad \Theta(X, \infty) = 0, \tag{24}$$

with $x = X$ and $0 < X \leqslant 1$.

Equation (24) expresses matching between the boundary-layer flow and the potential flow, which was considered in § 3.3. In view of (8) and (9), we expand the boundary-layer variables in terms of small Richardson numbers as follows:

$$U = 1 - nRi\ln|Ri|U_1(X, Y) + Ri[U_{2c}(X, Y) + U_{2h}(X, Y)] + \dots, \tag{25}$$

$$V = -nRi\ln|Ri|V_1(X, Y) + Ri[V_{2c}(X, Y) + V_{2h}(X, Y)] + \dots, \tag{26}$$

$$P = -nRi\ln|Ri|P_1(X, Y) + Ri[P_{2c}(X, Y) + P_{2h}(X, Y)] + \dots, \tag{27}$$

$$\Theta = \Theta_0(X, Y) - nRi\ln|Ri|\Theta_1(X, Y) + Ri[\Theta_{2c}(X, Y) + \Theta_{2h}(X, Y)] + \dots. \tag{28}$$

In order to facilitate the physical interpretation of the results to be given below, the terms of order $O(Ri)$ have been split into two parts, the first one being associated with circulation (subscript c), the second one being due to the hydrostatic pressure perturbation (subscript h). The terms of the order $O(Ri\ln|Ri|)$ are solely due to circulation.

The leading terms of the expansions (25) and (28) describe forced convection flow for $Pr = 0$, i.e. uniform flow with the well-known self-similar temperature distribution

$$\Theta_0 = \mathrm{erfc}(\eta) \quad \text{with} \quad \eta = Y/2\sqrt{X}, \tag{29}$$

cf. Schlichting & Gersten 2000, p. 216. Thus, the non-dimensional overall heat flow rate in the undisturbed forced flow is given by the relationship

$$-\int_0^1 \Theta_0'(0)X^{-1/2}\,\mathrm{d}X = 4/\sqrt{\pi}. \tag{30}$$

This result may be used to express the Richardson number in terms of the (given) plate temperature. Rewriting (4) in terms of the present non-dimensional variables and making use of (30) gives

$$Ri = (4/\sqrt{\pi})g\beta(T_p - T_\infty)(\alpha L)^{1/2}u_\infty^{-5/2} = (4/\sqrt{\pi})Ar/\sqrt{Pe}. \tag{31}$$

4.2. *Solutions*

The boundary-layer equations (19) to (22) and the boundary conditions (23) and (24) are expanded according to (25) to (28). Taking the first-order solution (29) into account, the following solutions for the velocity and pressure perturbations, respectively, are found:

$$-U_1 = P_1 = \frac{1}{2\pi}\sqrt{\frac{1-X}{X}}, \qquad V_1 = 2\sqrt{X}\eta P_1'(X), \tag{32}$$

$$-U_{2c} = P_{2c} = \tfrac{1}{2}\gamma(X), \qquad V_{2c} = 2\sqrt{X}\eta P_2'(X), \tag{33}$$

$$-U_{2h} = P_{2h} = \tfrac{1}{2}\sqrt{\pi X}[\eta \mathrm{erfc}(\eta) - (1/\sqrt{\pi})\exp(-\eta^2)], \qquad V_{2h} = -(\sqrt{\pi}/4)\,\mathrm{erf}(\eta), \tag{34}$$

with γ as defined in (10) and shown in figure 3. Primes indicate derivatives. For the hydrostatic pressure perturbation at the trailing edge, i.e. for $X=1$ and $\eta=0+$, equation (34) gives the value $P_{2h}=-1/2$, which is exactly compensated by the induced pressure perturbation P_{2c} as obtained from (33) with $\gamma(0)=1$, cf. Appendix C or figure 3. This is in accord with the Kutta condition.

For the three terms of the temperature perturbation, the following partial differential equations, written in terms of the linear differential operator

$$\mathrm{D} = \frac{\partial^2}{\partial \eta^2} + 2\eta\frac{\partial}{\partial \eta} - 4X\frac{\partial}{\partial X}, \tag{35}$$

are obtained:

$$\mathrm{D}(\Theta_1) = -(4/\sqrt{\pi})\eta\exp(-\eta^2)[P_1(X) + 2XP_1'(X)], \tag{36}$$

$$\mathrm{D}(\Theta_{2c}) = -(2/\sqrt{\pi})\eta\exp(-\eta^2)[\gamma(X) + 2X\gamma'(X)], \tag{37}$$

$$\mathrm{D}(\Theta_{2h}) = \sqrt{X}\exp(-\eta^2)F(\eta), \tag{38}$$

where

$$F(\eta) = (2/\sqrt{\pi})\eta\exp(-\eta^2) - 2\eta^2 + (1+2\eta^2)\,\mathrm{erf}(\eta). \tag{39}$$

Separating the variables, we can reduce (36) to (38) with boundary conditions

$$\Theta_1 = \Theta_{2c} = \Theta_{2h} = 0 \quad \text{on} \quad \eta = 0, \tag{40}$$

$$\Theta_1 = \Theta_{2c} = \Theta_{2h} = 0 \quad \text{as} \quad \eta \to \infty, \tag{41}$$

to ordinary differential equations that can be solved in closed form by standard methods. A free constant of integration is determined such as to avoid a singularity at $X=0$, which would give an infinite overall heat flow rate. The results are:

$$\Theta_1 = X^{-1}[\sqrt{X(1-X)} - \arcsin\sqrt{X}]\tilde{\Theta}_1(\eta), \tag{42}$$

$$\Theta_{2c} = g(X)\tilde{\Theta}_{2c}(\eta), \tag{43}$$

$$\Theta_{2h} = \tfrac{1}{4}\sqrt{\pi X}\;\tilde{\Theta}_{2h}(\eta), \tag{44}$$

where

$$g(X) = \gamma(X) - \frac{1}{2X}\int_0^X \gamma(\bar{X})\,\mathrm{d}\bar{X}; \tag{45}$$

$$\tilde{\Theta}_1(\eta) = \tfrac{1}{2}\pi^{-3/2}\eta\exp(-\eta^2), \qquad \tilde{\Theta}_{2c}(\eta) = \pi^{-1/2}\eta\exp(-\eta^2), \tag{46}$$

$$\tilde{\Theta}_{2h}(\eta) = \eta\left[H(\eta)\int_0^\eta F(\bar{\eta})\bar{\eta}\,\mathrm{d}\bar{\eta} + \int_\eta^\infty H(\bar{\eta})F(\bar{\eta})\bar{\eta}\,\mathrm{d}\bar{\eta}\right], \tag{47}$$

with

$$H(\eta) = \sqrt{\pi}\mathrm{erfc}(\eta) - (1/\eta)\exp(-\eta^2). \tag{48}$$

The functions defined in (45), (46) and (47) are shown in figures 3 and 5, respectively. The hydrostatic part of the present closed-form solution, i.e. (44) together with (47) and (48), is in accord with the numerical solution given by Leal (1973) for a semi-infinite plate, implying an outer flow without circulation. With respect to the heat-transfer calculation, see below, of particular interest is the derivative at the plate surface. From (47) and (48), we can deduce, perhaps a little surprisingly, the following

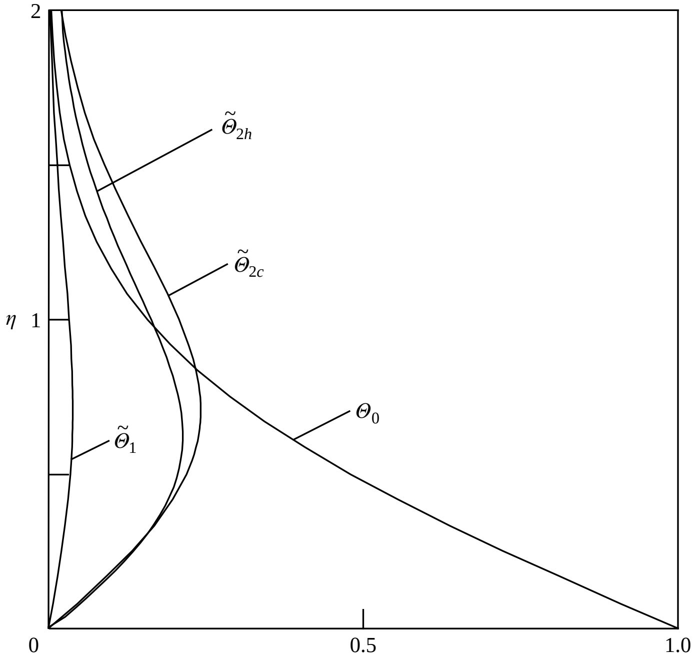

FIGURE 5. Self-similar temperature profiles.

exact value (Savić 2003, personal communication):

$$\tilde{\Theta}'_{2h}(0) = \int_0^\infty H(\bar{\eta})F(\bar{\eta})\bar{\eta}\,\mathrm{d}\bar{\eta} = -\tfrac{1}{2}. \tag{49}$$

Though $\gamma(X)$ is singular at the leading edge, $g(X)$ remains finite. The singular terms cancel, as can be seen by inserting the expansion (12) into (45). This gives

$$g(X) = \frac{4-\ln 4}{3\pi}\sqrt{X} + \dots \qquad (\text{for } X \ll 1). \tag{50}$$

4.3. *Buoyancy force*

The total buoyancy force is determined by integrating the hydrostatic pressure perturbation, i.e. $Ri\,P_{2h}$ according to (34), over the whole plate, taking into account both the upper and lower sides of the plate. Referring the force to the free-stream stagnation pressure and to the plate area, we obtain

$$C_B = -4Ri\int_0^1 P_{2h}(X, 0+)\,\mathrm{d}X = \tfrac{4}{3}Ri \tag{51}$$

for the buoyancy force coefficient, C_B.

4.4. *Heat transfer results*

The local Nusselt number, Nu_X, is defined as usual, i.e. $\mathrm{Nu}_X = \dot{q}LX/k(T_p - T_\infty)$ in terms of the local heat flux, $\dot{q}$, at the upper surface of the plate. The thermal conductivity k is assumed to be constant. Applying Fourier's law, expanding according to (28) for small Richardson numbers and using the results of § 4.2, we obtain

$$Nu_X = \sqrt{PeX/\pi}\big[1 - nRi\ln|Ri|Nu_X^{(1)} + Ri\big(Nu_X^{(2c)} + Nu_X^{(2h)}\big)\big], \tag{52}$$

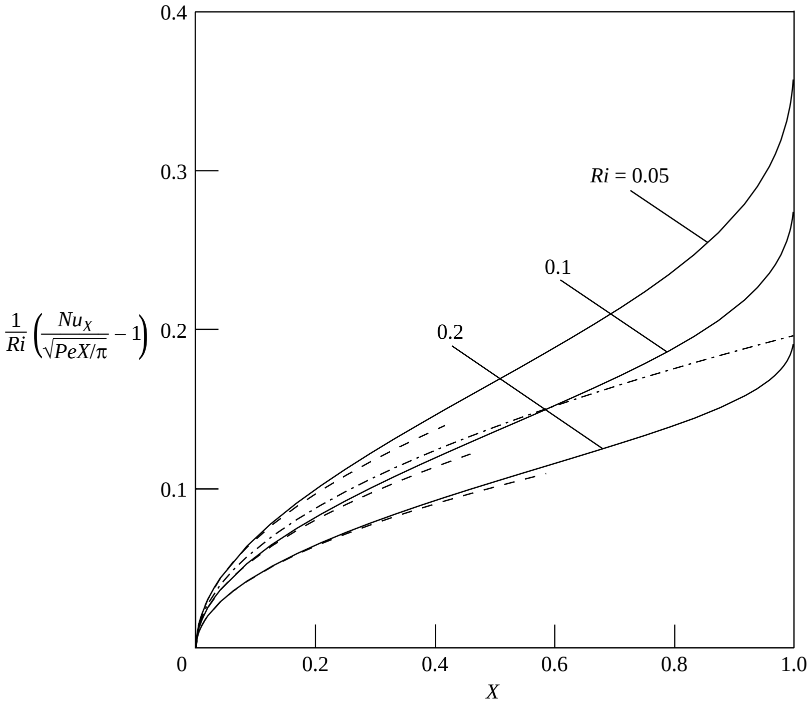

FIGURE 6. Perturbation of the local Nusselt number due to buoyancy for various values of the Richardson number Ri and $n = 1$. Solid lines: plate of finite length; dashed-dotted line: semi-infinite plate. Also shown: asymptotic expansions for $X \ll 1$ according to (56) (dashed lines).

where

$$Nu_X^{(1)} = (1/4\pi X)[\arcsin\sqrt{X} - \sqrt{X(1-X)}], \tag{53}$$

$$Nu_X^{(2c)} = -(1/2)g(X), \tag{54}$$

$$Nu_X^{(2h)} = (\pi/16)\sqrt{X}, \tag{55}$$

with $g(X)$ as defined in (45). The term $\sqrt{Pe\,X/\pi}$ is in accord with the classical forced-convection result. As indicated by the superscripts, $Nu_X^{(2h)}$ is due to the hydrostatic pressure perturbation, whereas $Nu_X^{(1)}$ and $Nu_X^{(2c)}$ are due to circulation. The latter terms are absent in the case of a semi-infinite plate. The perturbation of the Nusselt number according to (52) to (55) is shown in figure 6. For the purpose of comparison the well-known result for the semi-infinite plate is also shown.

Since the velocity perturbation is infinite at the leading edge, cf. (9) together with (8) and (12), we might also expect a singular behaviour of the Nusselt number. Expanding (53) and inserting the expansion (12) into (54) shows, however, that the singular terms cancel.† Hence one obtains

$$Nu_X = \sqrt{PeX/\pi}\left[1+(Ri/3\pi)\left(-\tfrac{1}{2}n\ln|Ri|+\ln 2-2+3\pi^2/16\right)\sqrt{X}+\ldots\right] \quad (X \ll 1), \tag{56}$$

† In a previous analysis of the mixed convection flow past a finite horizontal plate (Schneider 2000), the singular terms did not cancel owing to an algebraic error, i.e. there ought to be a minus rather than a plus sign on the right-hand side of the previous equation (8) and, as a consequence, the expansions (19) to (21) given by Schneider (2000) are incorrect.

i.e. the perturbation of the Nusselt number vanishes at the leading edge. The result (56) may be useful for determining the Nusselt number near the leading edge without recourse to numerical evaluations of the integrals, cf. figure 6 for comparisons. The term $3\pi^2/16$ in (56) is due to the hydrostatic pressure perturbation. It is the only term present in the case of a semi-infinite plate. The sum of the other perturbation terms gives the effect of the potential flow induced at a plate of finite length. This sum is positive or negative depending on whether $|Ri|$ is smaller or larger than $\exp[-(4 - \ln 4)/n]$, i.e. 7.33×10^{-2} for $n = 1$.

5. Conclusions and discussion

The results show that the flow past a heated or cooled horizontal plate of finite length is affected by buoyancy in a way that differs substantially from the well-known case of a semi-infinite plate. The primary effect is an induced potential flow with circulation. As a consequence, the influence of the trailing edge is not – as in other cases of boundary-layer flow – confined to a small region near the trailing edge, but covers the whole plate.

The buoyancy-induced potential flow gives rise to both normal (lift) and tangential (thrust) forces that resemble the forces observed at inclined flat plates in isothermal flow. The present analysis has been restricted to weak buoyancy effects, i.e. small Richardson numbers, in order to avoid boundary-layer separation and other effects that are beyond the scope of the present work. To deal with singularities associated with an unbounded flow field, sidewalls parallel to the plate have been introduced at distances that grow algebraically beyond bounds as the Richardson number Ri, which is defined in terms of the overall heat flow rate, tends to zero. Analytical results for the force coefficients have been obtained for laminar flow with large Péclet numbers and small Prandtl numbers as well as for turbulent flows with large Reynolds numbers. The results depend on the overall heat supply only, whereas details of the temperature distribution and/or the heat flux distribution at the plate are of negligible relevance. The lift and thrust coefficients are found to be of the order of $Ri \ln|Ri|$ and $(Ri \ln|Ri|)^2$, respectively. These orders of magnitude are applicable to both laminar and turbulent flow with the exception of laminar flow of a fluid with very large Prandtl number, as, in the latter case, the thermal boundary layer is embedded in a viscous boundary layer of much larger thickness.

The lift force competes with the buoyancy force, which is due to the hydrostatic pressure perturbation and points in the opposite direction. The value of the buoyancy force coefficient, C_B, depends on details of the heat transfer at the plate. For the particular case of constant wall temperature in laminar flow with vanishing Prandtl number, an analytical solution has been given in § 4.3, and other classical cases, e.g. constant wall heat flux, can be treated similarly on the basis of well-known solutions for the temperature distribution in forced flow. For more general cases, an upper bound for C_B can be given as follows. As the boundary-layer thickness increases monotonically with increasing distance from the leading edge, the hydrostatic pressure perturbation at the plate surface also increases monotonically until it reaches its trailing-edge value. Since the pressure is continuous at the trailing edge, the trailing-edge value of the hydrostatic pressure perturbation is $\mp Ri/2$ at the upper and lower surface, respectively, in the present non-dimensional notation, cf. (6). Accounting for the contributions from both the upper and lower sides of the plate, and observing that the pressure is referred to twice the free-stream stagnation pressure, it follows that C_B cannot exceed the value $2Ri$. On the other hand, (14) and (15) show that C_L is always smaller than $-2Ri$, cf. also figure 4. Thus, the lift force, which is directed opposite to the buoyancy force, exceeds the buoyancy force in magnitude, and the normal force coefficient, $C_n = C_B + C_L$, is negative for positive Richardson numbers, indicating that the net normal force exerted by a normal fluid ($\beta > 0$) on a heated plate of finite length is directed downward. For a cooled plate ($T_p < T_\infty$), all signs are inverted, of course, for symmetry reasons.

Concerning the tangential forces acting on the plate, it is well-known that the drag coefficient C_D decreases with increasing Reynolds number *Re* both for laminar and turbulent flow. The suction-force coefficient C_S, on the other hand, depends on the Richardson number only. Thus, the force due to leading-edge suction exceeds the viscous drag force in magnitude if the Reynolds number is sufficiently large, giving rise to a net tangential force that is in the opposite direction to the free stream. This effect may be added to the various means of generating thrust by supplying heat at the surface of an airfoil, as surveyed by Bartlmä (1975), Broadbent (1976) and Zierep (1980, 1990). A word of caution is in order, however. The singularity at the leading edge not only violates the assumption of small perturbations; it may also be associated, in reality, with various flow phenomena not taken into account in the present analysis, e.g. boundary-layer separation and cavitation. A suitably shaped, round leading edge might help to prevent the occurrence of such phenomena.

In view of the strong effect of the finite length of the plate on the velocity distribution, it appears advisable to reconsider the stability of the mixed convection flow over horizontal plates, following the way paved by previous investigators (e.g. Wu & Cheng 1976; Chen & Mucoglu 1979; Moutsoglou *et al.* 1981; Lee *et al.* 1992; Hall & Morris 1992).

As far as the heat transfer is concerned, the largest perturbation terms cancel. As a result, the effect of the finite length of the plate on the heat transfer is rather modest, the sign depending on the value of the Richardson number.

The present analysis ceases to be valid near the trailing edge, where the boundary layers interact with the potential flow. A problem related to the present one concerns the forced flow past an inclined flat plate, where the interaction leads to modifications of the Kutta condition and gives rise to a disturbance of symmetry of the potential flow (cf. Brown & Stewartson 1970; Chow & Melnik 1976; Smith 1983; and the survey by Kluwick 1998). Thus, future investigations of the trailing-edge problem in mixed convection flow past a horizontal plate are certainly desirable.

The author is grateful to Professor A. Kluwick for numerous suggestions, including references, and to Professor H. Steinrück for fruitful discussions on the problem. Dr V. Noshadi deserves credit for having drawn the author's attention to peculiarities of Navier–Stokes solutions for mixed convection flow past horizontal plates. Mr Lj. Savić provided numerical solutions and graphs; his help in checking the analysis and eliminating errors is also gratefully acknowledged. Finally, the author is indebted to anonymous referees for their comments that led to various improvements of the paper.

This paper is dedicated to Professor Klaus Gersten on the occasion of his 75th birthday.

Appendix A. Justification for neglecting dissipation

A.1. *Laminar flow*

Making use of well-known relationships for laminar viscous wakes (cf. Schlichting & Gersten 2000, p. 189), the viscous dissipation, per units of time and length in the

x-direction, can be estimated to be of the order of $(C_D L)^2 \rho_\infty u_\infty^{7/2} \nu^{-1/2} x^{-3/2}$, where C_D is the drag coefficient of the plate and ν is the kinematic viscosity of the fluid. This shows that the effect of viscous dissipation decays as $x \to \infty$ and can, therefore, not affect the asymptotic behaviour of the wake-induced flow at infinity. Integrating over the whole wake, i.e. from x of the order of the plate length L to infinity, gives $C_D^2 \rho_\infty u_\infty^{7/2} L^{3/2} \nu^{-1/2}$ as the order of magnitude of the total viscous dissipation, D, per unit of time. This is to be compared with the total heat flow, $\dot{Q}_0$. Introducing the Richardson number according to (4), and observing that $C_D = O(Re^{-1/2})$ with $Re = u_\infty L/\nu$, we obtain

$$\frac{D}{\dot{Q}_0} = O\left(\frac{1}{Ri\sqrt{Re}} \frac{g\beta L}{c_p}\right). \tag{A 1}$$

The non-dimensional parameter $g\beta L/c_p$ is very small for liquid metals and reasonable plate lengths, e.g. about 2×10^{-6} for mercury and $L = 1$ m. Since the Reynolds number is assumed to be large, i.e. typically of the order of 10^4, dissipation is negligible even for extremely small values of the Richardson number.

A.2. *Turbulent flow*

The turbulent dissipation rate per unit of mass is approximately equal to $k^{3/2} l^{-1}$, where k is the turbulent kinetic energy per unit of mass and l is the integral length scale. In a turbulent wake, k and l are known to be of the order of the mean velocity defect squared and the wake width, respectively (cf. Tennekes & Lumley 1972). These quantities can be estimated with well-known relationships (cf. Schlichting & Gersten 2000, pp. 667, 668) to obtain $(C_D L)^{3/2} \rho_\infty u_\infty^3 x^{-3/2}$ as the order of magnitude of the turbulent dissipation per units of time and length in the x-direction. Thus, as in the laminar case, the effect of dissipation does not affect the asymptotic behaviour of the wake-induced flow at infinity. Integrating over the wake gives

$$\frac{D}{\dot{Q}_0} = O\left(\frac{C_D^{3/2}}{Ri} \frac{g\beta L}{c_p}\right). \tag{A 2}$$

As noted above, $g\beta L/c_p$ is very small, and since the drag coefficient C_D is also very small, i.e. about 5×10^{-3} for Reynolds numbers near the critical value and even smaller for very large Reynolds numbers, the dissipation rate is, as in the laminar case, negligible even for very small values of the Richardson number.

Appendix B. Potential-flow solution

The complex potential $f(z)$, with $z = x + \mathrm{i}y$, is introduced, and the solution will be given in terms of the strength of vortices distributed continuously in the plate $(0 < x \leqslant 1)$ and in the wake region $(x \geqslant 1)$, cf. figure 2. To satisfy the boundary conditions at the channel walls that are a distance $b/2$ each apart from the x-axis, the mirror method is applied. Thus, vortices of strength $Ri\tilde{\gamma}(x)$ are distributed on lines $y = \pm 2mb$, whereas vortices of strength $-Ri\tilde{\gamma}(x)$ are distributed on lines $y = \pm(2m+1)b$, with $m = 0, 1, 2, 3, \ldots$. This gives the following complex potential (with ξ being real):

$$f(z) = z - Ri\frac{\mathrm{i}}{2\pi}\int_0^\infty \tilde{\gamma}(\xi) \sum_{m=0}^{\infty} [\ln|z - \xi \pm 2mb\mathrm{i}| - \ln|z - \xi \pm \mathrm{i}(2m+1)b|]\, \mathrm{d}\xi. \tag{B 1}$$

Omitting the additive constants $\pm\ln(mb^2)$ as irrelevant for the potential, (B 1) may be written as

$$f(z)=z-Ri\frac{\mathrm{i}}{2\pi}\int_0^\infty \tilde{\gamma}(\xi)\left\{\ln\left|(z-\xi)\prod_{m=1}^{\infty}\left[1+\frac{(z-\xi)^2}{(2m)^2b^2}\right]\right| - \ln\left|\prod_{m=1}^{\infty}\left[1+\frac{(z-\xi)^2}{(2m-1)^2b^2}\right]\right|\right\}\mathrm{d}\xi. \quad \text{(B 2)}$$

Making use of well-known representations of hyperbolic functions in terms of infinite products (cf. Abramowitz & Stegun 1965) and omitting a further additive constant, (B 2) reduces to

$$f(z)=z-Ri\frac{\mathrm{i}}{2\pi}\int_0^\infty \tilde{\gamma}(\xi)\ln\left|\tanh\frac{\pi(z-\xi)}{2b}\right|\mathrm{d}\xi, \quad \text{(B 3)}$$

and the following integral representation is obtained for the complex velocity perturbation:

$$u-\mathrm{i}v=\frac{\mathrm{d}f}{\mathrm{d}z}=1-Ri\frac{\mathrm{i}}{2b}\int_0^\infty\frac{\tilde{\gamma}(\xi)\,\mathrm{d}\xi}{\sinh\left[\pi(z-\xi)/b\right]}. \quad \text{(B 4)}$$

Of particular interest are the velocity perturbations in the plane of the plate. Since $z\to x$ as $y\to 0$, (B 4) immediately gives the integral representation of the normal velocity component as follows:

$$v(x,0)=\frac{Ri}{2b}\int_0^\infty\frac{\tilde{\gamma}(\xi)\,\mathrm{d}\xi}{\sinh\left[\pi(x-\xi)/b\right]}. \quad \text{(B 5)}$$

Here, as well as in all similar integrals appearing in this paper, the Cauchy principal value is to be taken.

Concerning the tangential velocity component, we may observe that the imaginary part of the integrand in (B 4) vanishes as $y\to 0$, except if $\xi\to x$. Thus, $\tilde{\gamma}(\xi)$ can be replaced by $\tilde{\gamma}(x)$, and the remaining integral can be evaluated, making use of well-known relationships for hyperbolic functions, cf. Abramowitz & Stegun 1965. Together with the linearized Bernoulli equation this gives

$$u(x,0\pm)-1=-p(x,0\pm)=\mp\tfrac{1}{2}Ri\;\tilde{\gamma}(x). \quad \text{(B 6)}$$

This equation resembles the classical result for the potential flow past a plate in an unbounded domain, indicating that the effects of the channel-walls on the velocity perturbation in the plane of the plate cancel for symmetry reasons.

To determine the vortex strength distribution, $\tilde{\gamma}(x)$, the wake region is considered first. Comparing (B 6) with (6), we obtain

$$\tilde{\gamma}(x)\equiv 1 \qquad (x\geqslant 1). \quad \text{(B 7)}$$

At the plate, the boundary condition (7) has to be satisfied. On the basis of (B 5), this gives

$$\int_0^1\frac{\tilde{\gamma}(\xi)\,\mathrm{d}\xi}{\sinh\left[\pi(x-\xi)/b\right]}+\int_1^\infty\frac{\mathrm{d}\xi}{\sinh\left[\pi(x-\xi)/b\right]}=0. \quad \text{(B 8)}$$

With the help of well-known integral formulae (cf. Abramowitz & Stegun 1965), (B 8) becomes

$$\int_0^1\frac{\tilde{\gamma}(\xi)\,\mathrm{d}\xi}{\sinh\left[\pi(x-\xi)/b\right]}=-\frac{b}{\pi}\ln\left[\tanh\frac{\pi(1-x)}{2b}\right] \quad (0<x<1), \quad \text{(B 9)}$$

and upon expanding both the integrand and the right-hand side of (B 9) for $b \to \infty$, we obtain

$$\int_0^1 \frac{\tilde{\gamma}(\xi)\,\mathrm{d}\xi}{x-\xi} = \ln\frac{2b}{\pi(1-x)} \qquad (0 < x < 1). \tag{B 10}$$

This integral equation is of a type that is well known in aerodynamics (cf. Schneider 1978). The solution can be written as an integral of elementary functions as follows:

$$\tilde{\gamma}(x) = \gamma(x) + \frac{1}{\pi}\sqrt{\frac{1-x}{x}}\,\ln\frac{2\mathrm{b}}{\pi} \qquad (0 < x < 1), \tag{B 11}$$

with $\gamma(x)$ as given in (10). Equations (B 6) and (B 11) with $b = (\pi/2)|Ri|^{-n}$ lead to (8) and (9).

Appendix C. Vortex strength at the trailing edge

Rather than expanding the solution (10) for $x = 1 - \delta$, with $\delta \to 0$, which is a little cumbersome, it is more convenient to start from the integral equation (B 10). Upon introducing $x = 1 - \delta$, we obtain

$$\int_0^1 \frac{\tilde{\gamma}(\xi)\,\mathrm{d}\xi}{1-\delta-\xi} = \ln\frac{2b}{\pi\delta}, \tag{C 1}$$

which can also be written as

$$\tilde{\gamma}(1)\int_0^1 \frac{\mathrm{d}\xi}{1-\delta-\xi} + \int_0^1 \frac{\tilde{\gamma}(\xi)-\tilde{\gamma}(1)}{1-\delta-\xi}\,\mathrm{d}\xi = -\ln\delta + \ln\frac{2b}{\pi}. \tag{C 2}$$

The first integral can easily be evaluated as $-\ln\delta + \ln(1-\delta)$, which reduces to $-\ln\delta$ as $\delta \to 0$. Since the second integral and the term $\ln(2b/\pi)$ remain finite as $\delta \to 0$, it follows from (C 2) that $\tilde{\gamma}(1) = 1$. Furthermore, $\gamma(1) = 1$, as can be seen from (B 11).

Appendix D. Effects of the break-down of the boundary-layer analysis far downstream

It is well known (cf. Schlichting & Gersten 2000, pp. 187–190, 667–669) that the wake thickness increases proportional to $\sqrt{x}$. Thus, sufficiently far downstream, the thermal wake thickness, Δ, becomes comparable to the cannel width, which is of the order of $|Ri|^{-n}$, and the boundary-layer analysis ceases to be valid. To be more specific, we consider laminar and turbulent flows separately.

For laminar flow, $\Delta(x)$ is of the order of $\sqrt{x/Pe}$, where Pe is the Péclet number. Thus, the boundary-layer analysis is inapplicable for values of x that are of the order of, or larger than, $x*$, with

$$x* = Pe\,|Ri|^{-2n} \to \infty \quad \text{as} \quad Ri \to 0, \quad Pe \to \infty. \tag{D 1}$$

For turbulent flow, the estimate is a little more elaborate. According to Schlichting & Gersten (2000, pp. 667–669), the wake thickness $\Delta(x)$ is of the order of $(|\dot{Q}_0|x/\rho_\infty u_\infty c_p T_\infty L)^{1/2}$ (in the present notation). To relate this expression to the Reynolds number Re, the Stanton number $St = \dot{Q}_0/\rho_\infty u_\infty c_p(T_p - T_\infty)L$ is introduced, with T_p denoting a characteristic value of the plate temperature. Taking into account that the Stanton number is of the order of the wall-friction coefficient, which is as small as $(\ln Re)^{-2}$ (cf. Schlichting & Gersten 2000, pp. 605, 581), we obtain that the wake thickness is comparable to the channel width for values of x that are of the order of, or larger than, $x*$, with

$$x* = (\ln Re)^2 |Ri|^{-2n} T_\infty |T_p - T_\infty|^{-1} \to \infty \quad \text{as } Ri \to 0, \quad Re \to \infty. \tag{D 2}$$

Since the vortex sheet representing the wake extends to infinity, it remains to show that the wake region that is beyond the limits of applicability of the boundary-layer theory contributes very little to the potential. Expanding the integral in (B 3) for $\xi/b \to \infty$, while z/b is in the region of interest, i.e. $|z/b| = O(1)$, it is easily shown that the integrand is of the order of $\exp(-\pi\xi/b) = \exp(-2|Ri|^n \xi)$. Integrating from $\xi = x*$ to ∞ gives a term of the order of $|Ri|^{-n} \exp(-2|Ri|^n x*)$, which, in view of (D 1) and (D 2) for laminar and turbulent flow, respectively, is exponentially small in both cases.

REFERENCES

ABRAMOWITZ, M. & STEGUN, I. A. 1965 *Handbook of Mathematical Functions*, pp. 83–86. Dover.

BARTLMÄ, F. 1975 *Gasdynamik der Verbrennung*, pp. 137–197. Springer.

BROADBENT, E. G. 1976 Flows with heat addition. *Prog. Aerospace Sci.* **17**, 93–108.

BROWN, S. N. & STEWARTSON, K. 1970 Trailing edge stall. *J. Fluid Mech.* **42**, 561–584.

CHEN, T. S. & MUCOGLU, A. 1979 Wave instability of mixed convection flow over a horizontal flat plate. *Intl J. Heat Mass Transfer* **22**, 185–196.

CHOW, R. & MELNIK, R. E. 1976 Numerical solutions of the triple deck equations for laminar trailing-edge stall. *Grumman Res. Dept Rep.* RE-526J.

GERSTEN, K. & HERWIG, H. 1992 *Strömungsmechanik*. Vieweg, Braunschweig.

GERSTEN, K. & SCHILAWA, S. 1978 Buoyancy effects on forced-convection heat transfer in horizontal boundary layers. In *Proc. of the 6th Intl Heat Transfer Conf.* vol. 1, pp. 73–78. Hemisphere.

HALL, P. & MORRIS, H. 1992 On the instability of boundary layers on heated flat plates. *J. Fluid Mech.* **245**, 367–400.

HIEBER, C. A. 1973 Mixed convection above a heated horizontal surface. *Intl J. Heat Mass Transfer* **16**, 769–785.

HIGUERA, F. J. 1997 Opposing mixed convection flow in a wall jet over a horizontal plate. *J. Fluid Mech.* **342**, 355–375.

IMURA, H., GILPIN, R. R. & CHENG, K. C. 1978 An experimental investigation of heat transfer and buoyancy induced transition from laminar forced convection to turbulent free convection over a horizontal isothermally heated plate. *Trans. ASME* C*: J. Heat Transfer* **100**, 429–434.

KLUWICK, A. 1998 Interacting laminar and turbulent boundary layers. In *Recent Advances in Boundary Layer Theory* (ed. A. Kluwick). CISM Courses and Lectures no. 390, pp. 231–330, Springer.

LAGRÉE, P.-Y. 2001 Removing the marching breakdown of the boundary-layer equations for mixed convection above a horizontal plate. *Intl J. Heat Mass Transfer* **44**, 3359–3372.

LEAL, L. G. 1973 Combined forced and free convection heat transfer from a horizontal plate. *Z. Angew. Math. Phys.* **24**, 20–42.

LEE, H. R., CHEN, T. S. & ARMALY, B. F. 1992 Nonparallel thermal instability of mixed convection flow on nonisothermal horizontal and inclined flat plates. *Intl J. Heat Mass Transfer* **35**, 1913–1925.

MÖRWALD, K. 1988 Asymptotische Theorie freier turbulenter Scherströmungen. Doctoral thesis, Technical University of Vienna.

MOUTSOGLOU, A., CHEN, T. S. & CHENG, K. C. 1981 Vortex instability of mixed convection flow over a horizontal flat plate. *Trans. ASME* C*: J. Heat Transfer* **103**, 257–261.

OSWATITSCH, K. 1976 *Grundlagen der Gasdynamik*, pp. 447–450. Springer.

ROBERTSON, G. E., SEINFELD, J. H. & LEAL, L. G. 1973 Combined forced and free convection flow past a horizontal flat plate. *AIChE J.* **19**, 998–1008.

SCHLICHTING, H. & GERSTEN, K. 2000 *Boundary Layer Theory*, 8th edn. Springer.

SCHNEIDER, W. 1978 *Mathematische Methoden der Strömungsmechanik*, pp. 142–145. Vieweg.

Schneider, W. 1991 Boundary-layer theory of free turbulent shear flows. *Z. Flugwiss. Weltraumforsch.* **15**, 143–158.

Schneider, W. 2000 Mixed convection at a finite horizontal plate. In *Proc. of the Third European Thermal Sci. Conf.* (ed. E. W. P. Hahne, W. Heidemann & K. Spindler), pp. 195–198. Edizioni EPS, Pisa.

Schneider, W. 2001 Peculiarities of boundary-layer flows over horizontal plates. In *Applicable Mathematics – Its Perspectives and Challenges* (ed. J. C. Misra), pp. 118–123. Narosa, New Delhi.

Schneider, W. & Wasel, M. G. 1985 Breakdown of the boundary-layer approximation for mixed convection above a horizontal plate. *Intl J. Heat Mass Transfer* **28**, 2307–2313.

Smith, F. T. 1983 Interacting flow and trailing edge separation – no stall. *J. Fluid Mech.* **131**, 219–249.

Steinrück, H. 1994 Mixed convection over a cooled horizontal plate: non-uniqueness and numerical instabilities of the boundary-layer equations. *J. Fluid Mech.* **278**, 251–265.

Steinrück, H. 2001 A review of the mixed convection boundary-layer flow over a horizontal cooled plate. *GAMM-Mitteilungen* 2001/2, 127–158.

Taylor, G. I. 1958 Flow induced by jets. *J. Aero/Space Sci.* **25**, 464–465.

Tennekes, H. & Lumley, J. L. 1972 *A First Course in Turbulence*, p. 113. MIT Press, Cambridge, MA.

Wang, X. A. 1982 An experimental study of mixed, forced, and free convection heat transfer from a horizontal flat plate to air. *Trans. ASME* C*: J. Heat Transfer* **104**, 139–144.

Wickern, G. 1991 Mixed convection from an arbitrarily inclined semi-infinite flat plate – II. The influence of the Prandtl number. *Intl J. Heat Mass Transfer* **34**, 1947–1957.

Wu, R.-S. & Cheng, K. C. 1976 Thermal instability of Blasius flow along horizontal plates. *Intl J. Heat Mass Transfer* **19**, 907–913.

Zierep, J. 1980 Theory of flows in compressible media with heat addition. *Fluid Dyn. Trans.* **10**, 213–240.

Zierep, J. 1990 *Strömungen mit Energiezufuhr*, 2nd edn, pp. 43–94. G. Braun, Karlsruhe.